

Phosphatidylinositol (4,5)-Bisphosphate Regulation of N-Methyl-D-aspartate Receptor Channels in Cortical Neurons

Madhuchhanda Mandal and Zhen Yan

Department of Physiology & Biophysics, State University of New York at Buffalo, Buffalo, New York

Received June 19, 2009; accepted September 18, 2009

ABSTRACT

The membrane phospholipid phosphatidylinositol (4,5)-bisphosphate (PIP₂) has been implicated in the regulation of several ion channels and transporters. In this study, we examined the impact of PIP₂ on N-methyl-D-aspartate receptors (NMDARs) in cortical neurons. Blocking PIP₂ synthesis by inhibiting phosphoinositide-4 kinase, or stimulating PIP₂ hydrolysis via activation of phospholipase C (PLC), or blocking PIP₂ function with an antibody caused a significant reduction of NMDAR-mediated currents. On the other hand, inhibition of PLC or application of PIP₂ caused an enhancement of NMDAR currents. These electrophysiological effects were accompanied by changes in NMDAR surface clusters induced by agents that manipulate PIP₂ levels. The PIP₂ regulation of NMDAR currents was abolished by the dynamin inhibitory peptide, which blocks receptor internalization. Agents perturbing actin stability pre-

vented PIP₂ regulation of NMDAR currents, suggesting the actin-dependence of this effect of PIP₂. Cofilin, a major actin depolymerizing factor, which has a common binding sequence for actin and PIP₂, was required for PIP₂ regulation of NMDAR currents. It is noteworthy that the PIP₂ regulation of NMDAR channels was impaired in a transgenic mouse model of Alzheimer's disease, probably because of the amyloid- β disruption of PIP₂ metabolism. Taken together, our data suggest that continuous synthesis of PIP₂ at the membrane might be important for the maintenance of NMDARs at the cell surface. When PIP₂ is lost, cofilin is released from the PIP₂ complex and is rendered free to depolymerize actin. With the actin cytoskeleton no longer intact, NMDARs are internalized via a dynamin/clathrin-dependent mechanism, leading to reduced NMDAR currents.

The N-methyl-D-aspartate receptor (NMDAR), one of the major glutamate receptor channels in central neurons, plays a key role in multiple neuronal functions, including synapse formation, synaptic plasticity, learning, and memory. Dysregulation of NMDARs has been implicated in ischemia, epilepsy, and neuropsychiatric disorders (Dingledine et al., 1999; Lau and Zukin, 2007). Synaptic targeting and incorporation of NMDA receptors are dynamically regulated (Wenthold et al., 2003). After being released from the endoplasmic reticulum, NMDARs are rapidly transported along microtubule tracks in dendritic shafts (Washbourne et al., 2002; Yuen et al., 2005), followed by being delivered to actin-

rich dendritic spines. NMDARs are tethered to actin cytoskeleton via scaffolding and adaptor proteins, such as α -actinin and postsynaptic density-95 (Wyszynski et al., 1997; Pak et al., 2001). Several mechanisms have been proposed to be important for stabilizing and/or promoting surface NMDA receptor expression, including the PDZ domain-mediated interactions between NR2 subunits and postsynaptic density-95 (Kornau et al., 1995; Roche et al., 2001; Lin et al., 2004) and tyrosine dephosphorylation of NR2 subunits that triggers clathrin-dependent endocytosis (Vissel et al., 2001; Prybylowski et al., 2005). Actin dynamics also plays a key role in controlling NMDAR trafficking and function, because actin depolymerization reduces NMDA channel activity (Rosenmund and Westbrook, 1993), decreases the number of synaptic NMDAR clusters (Allison et al., 1998), and triggers long-term depression of NMDA synaptic responses in hippocampus (Morishita et al., 2005).

Phosphatidylinositol-4,5-bisphosphate (PIP₂) is a pro-

This work was supported by the National Institutes of Health National Institute on Aging [Grant AG21923] and the National Institutes of Health National Institute of Mental Health [Grant MH84233].

Article, publication date, and citation information can be found at <http://molpharm.aspetjournals.org>.

doi:10.1124/mol.109.058701.

ABBREVIATIONS: NMDAR, N-methyl-D-aspartate receptor; NMDA, N-methyl-D-aspartate; PIP₂, phosphatidylinositol (4,5)-bisphosphate; PLC, phospholipase C; IP₃, inositol 1,4,5-triphosphate; PI-4 kinase, phosphatidylinositol-4 kinase; EPSC, excitatory postsynaptic current; AD, Alzheimer's disease; A β : amyloid- β ; APP: β -amyloid precursor protein; ANOVA, analysis of variance; DAG, diacylglycerol; CCh, carbachol; PBS, phosphate-buffered saline; PAO, phenyl arsine oxide; DMSO, dimethyl sulfoxide; PI, phosphatidylinositol; BAPTA, 1,2-bis(2-aminophenoxy)ethane-N,N,N',N'-tetraacetic acid; mAChR, muscarinic acetylcholine receptor; U73122, 1-[6-[[17 β -methoxyestra-1,3,5(10)-trien-17-yl]-amino]hexyl]-1H-pyrrole-2,5-dione; U73343, 1-[6-[[17 β -3-methoxyestra-1,3,5(10)-trien-17-yl]amino]hexyl]-2,5-pyrrolidine-dione; QX-314, N-(2,6-dimethylphenyl)carbamoymethyl)triethylammonium bromide.

foundly versatile membrane phospholipid synthesized by the progressive phosphorylation of the cell-membrane phosphoinositides (Toker, 1998). Although present in very small quantities, accounting for only 1% of the total acidic membrane lipid, the dynamic change of PIP₂ concentration is known to affect many membrane proteins, including transporters and ion channels (Suh and Hille, 2005). Much evidence of this regulation has been obtained from studies on voltage-gated ion channels. K⁺ channels are most extensively studied in this respect: ATP-sensitive K_{ATP} channels, inward rectifying K⁺ channels, G protein-gated inwardly rectifying channels, and members of the KCNQ family all require the constant synthesis of PIP₂ at the membrane for their full functionality (Hilgemann and Ball, 1996; Huang et al., 1998; Kobrinisky et al., 2000; Zhang et al., 2003). Voltage-gated Ca²⁺ channels, epithelial Na⁺ channels, and sensory transduction channels of the TRP family are also regulated by PIP₂ (Wu et al., 2002; Prescott and Julius, 2003; Kunzelmann et al., 2005; Liu and Qin, 2005; Albert et al., 2008).

Despite numerous reports on PIP₂ regulation of voltage-gated ion channels, the impact of PIP₂ on ligand-gated ion channels is largely unknown. It has been found that NMDAR activation during synaptic plasticity stimulates PIP₂ hydrolysis by PLC, causing the loss of PSD scaffolding proteins and actin depolymerization in dendritic spines (Horne and Dell'Acqua, 2007), but it is unclear whether the increase or decrease of cellular PIP₂ content affects NMDAR trafficking and function. By mainly using the *Xenopus laevis* oocyte expression system, it has been shown that PIP₂ modulates NMDAR activity through α -actinin (Michailidis et al., 2007), whose actin-regulating function requires PIP₂ (Fukami et al., 1992). In this study, we have provided evidence showing that PIP₂ facilitates NMDAR surface expression in native neurons, and loss of PIP₂ enhances clathrin/dynamin-dependent NMDAR internalization by promoting cofilin depolymerization of actin cytoskeleton. Moreover, we have found that the PIP₂ regulation of NMDARs is impaired by β -amyloid, suggesting that the altered PIP₂ metabolism in AD (Berman et al., 2008) may contribute to the synaptic dysfunction and cognitive decline via aberrant NMDAR signaling.

Materials and Methods

Materials. Purified PIP₂ was obtained from Calbiochem (San Diego, CA). Anti-PIP₂ antibody was from Assay Designs (Ann Arbor, MI), and anti-cofilin antibody was from Cell Signaling Technology (Danvers, MA). Latrunculin B, phalloidin, wortmannin, phenyl arsine oxide (PAO), and carbachol were obtained from Sigma-Aldrich (St. Louis, MO). U73122, U73343, and dynamin inhibitory peptide were obtained from Tocris Cookson (Ellisville, MO). Concentrated stocks of the reagents were made in DMSO or water and stored at -20°C. Stocks were thawed and diluted immediately before the experiment. The final concentration of DMSO did not exceed 0.1%. PIP₂ was diluted in distilled water (1 mg/ml) and sonicated for 15 min to form liposomes (20–200 nm) before application (Liu and Qin, 2005).

AD Model and A β Oligomer Preparation. β -Amyloid precursor protein (APP) transgenic mice carrying the Swedish mutation (K670N, M671L) were purchased from Taconic (Germantown, NY). Eight-week-old transgenic male mice (on B6SJLF1 hybrid background) were bred with mature B6SJLF1 female mice. Genotyping was performed by polymerase chain reaction according to the manufacturer's protocol.

Oligomeric A β _{1–42} was prepared as described previously (Dahl-

gren et al., 2002). In brief, the A β _{1–42} peptide (AnaSpec Inc., San Jose, CA) was dissolved in hexafluoroisopropanol to 1 mM. Hexafluoroisopropanol was then removed under vacuum. The remaining A β _{1–42} peptide was then resuspended in DMSO to 5 mM and diluted in H₂O to 100 μ M. The oligomeric A β was formed by incubating at 4°C for 24 h.

Acute Dissociation Procedure. Frontal cortical neurons were dissociated from young adult (3–4 weeks old) Sprague-Dawley rats or APP-transgenic mice (1-year-old) using procedures as described previously (Wang et al., 2003; Gu et al., 2009). All experiments were performed with the approval of the State University of Buffalo Animal Care Committee (Buffalo, NY). Brain slices were incubated in NaHCO₃-buffered saline, and then frontal cortex was dissected out and placed in an oxygenated chamber containing papain (0.8 mg/ml; Sigma-Aldrich) in Hanks' balanced salt solution (Sigma-Aldrich). After 40-min enzyme digestion at room temperature, the tissue was rinsed three times with low Ca²⁺, HEPES-buffered saline and mechanically dissociated with a graded series of fire-polished Pasteur pipettes. Immediately after dissociation, the cell suspension was plated into a 35-mm Lux Petri dish, which was then placed on the stage of a Nikon inverted microscope (Nikon, Tokyo, Japan). Ionic currents were measured 5 min after the initiation of whole-cell recordings. Each cell was recorded for 20 to 30 min.

Primary Neuronal Culture. Rat frontal cortical cultures were prepared by methods described previously (Gu et al., 2009). In brief, frontal cortex was dissected from 18-day rat embryos, and cells were dissociated using trypsin and trituration through a Pasteur pipette. Neurons were plated on coverslips coated with poly(L-lysine) in Dulbecco's modified Eagle's medium with 10% fetal calf serum with a density of 3 \times 10⁴ cells/cm². When neurons were attached to the coverslip within 24 h, the medium was changed to Neurobasal medium with B27 supplement. Neurons were maintained for 3 to 4 weeks before being used for immunostaining.

Whole-Cell Recording of Ionic Currents. Recordings of whole-cell NMDA-elicited ionic currents used standard voltage-clamp techniques (Wang et al., 2003). The internal solution consisted of 180 mM N-methyl-D-glucamine, 40 mM HEPES, 4 mM MgCl₂, 0.1 mM BAPTA, 12 mM phosphocreatine, 3 mM Na₂ATP, 0.5 mM Na₂GTP, and 0.1 mM leupeptin, pH 7.2 to 7.3 (adjusted with H₂SO₄), 265 to 270 mOsm. The external solution consisted of 127 mM NaCl, 20 mM CsCl, 10 mM HEPES, 1 mM CaCl₂, 5 mM BaCl₂, 12 mM glucose, 0.001 mM tetrodotoxin, and 0.02 mM glycine, pH 7.3 to 7.4, 300 to 305 mOsm. Recordings were obtained with an Axopatch 200B patch-clamp amplifier (Molecular Devices, Sunnyvale, CA) that was controlled by an IBM personal computer running pCLAMP (version 8) with a DigiData 1320 series interface (Molecular Devices). Electrode resistances were typically 2 to 4 M Ω in the bath. After seal rupture, series resistance (4–10 M Ω) was compensated (70–90%) and periodically monitored. The cell membrane potential was held at -60 mV. NMDA (100 μ M) was applied for 2 s every 30 s to minimize desensitization-induced decrease of current amplitude. Drugs were applied with a gravity-fed "sewer pipe" system. The array of application capillaries (150 μ m inner diameter) was positioned a few hundred microns from the cell under study. Solution changes were affected by the SF-77B fast-step solution stimulus delivery device (Warner Instruments, Hamden, CT). Recordings were performed at room temperature. Data analyses were performed with AxoGraph (Molecular Devices) and KaleidaGraph (Albeck Software, Reading, PA). Student *t* tests or ANOVA tests were performed to compare the differential degrees of current modulation between groups subjected to different treatment.

Electrophysiological Recordings in Slices. NMDAR-mediated synaptic currents in cortical slices were recorded using the whole-cell voltage-clamp recording technique (Wang et al., 2003; Gu et al., 2009). The slice (300 μ m) was placed in a perfusion chamber attached to the fixed-stage of an Olympus upright microscope (Olympus, Tokyo, Japan) and submerged in continuously flowing oxygenated artificial cerebrospinal fluid. Cells were visualized with a 40 \times

water-immersion lens and illuminated with near infrared light, and the image was detected with an infrared-sensitive charge-coupled device camera. A Multiclamp 700A amplifier was used for these recordings (Molecular Devices). Tight seals (2–10 G Ω) from visualized pyramidal neurons were obtained by applying negative pressure. The membrane was disrupted with additional suction, and the whole-cell configuration was obtained. The access resistances ranged from 13 to 18 M Ω . For NMDAR-EPSC recording, cells were bathed in artificial cerebrospinal fluid containing 6-cyano-2,3-dihydroxy-7-nitroquinoxaline (20 μ M) and bicuculline (10 μ M) to block α -amino-3-hydroxy-5-methyl-4-isoxazolepropionic acid/kainate receptors and GABA_A receptors, respectively. Electrodes (5–9 M Ω) were filled with the following internal solution: 130 mM cesium-methanesulfonate, 10 mM CsCl, 4 mM NaCl, 10 mM HEPES, 1 mM MgCl₂, 5 mM EGTA, 2.2 mM QX-314, 12 mM phosphocreatine, 5 mM Mg-ATP, 0.2 mM Na₂-GTP, and 0.1 mM leupeptin, pH 7.2 to 7.3, 265 to 270 mOsm. Evoked currents were generated with a 0.6-ms pulse from a stimulation isolation unit controlled by an S48 pulse generator (Astro-Med, West Warwick, RI). A bipolar stimulating electrode was positioned \sim 100 μ m from the neuron under recording. Before stimulation, cells (voltage-clamped at -70 mV) were depolarized to $+60$ mV for 3 s to fully relieve the voltage-dependent Mg²⁺ block of NMDAR channels. Slice recordings were performed at room temperature. Clampfit Program (Molecular Devices) was used to analyze evoked synaptic activity. For electrophysiological data, the drug-induced percentage change was calculated in each cell, and the average (mean \pm S.E.) of the percentage change in a sample of cells tested in each condition was given in the text.

Immunocytochemical Staining. Cultured neurons on coverslips (days in vitro 21–30) were treated with drugs as described in the text. After treatment, the drugs were washed off, and cells were fixed in 4% paraformaldehyde for 20 min at room temperature and washed three to five times with PBS. Neurons were then incubated with 5% bovine serum albumin for 1 h to block nonspecific staining. Next, neurons were labeled for surface NR1 clusters by incubating overnight at 4°C with anti-NR1 antibody directed against the extracellular loop (amino acids 660–811) of NR1 (clone 54.1, 1:500; Millipore Corporation, Billerica, MA). This NR1 antibody gave a single band at \sim 110 kDa in Western blot assays (Yuen et al., 2008) and

gave punctated signals on dendritic spines of cultured cortical neurons in immunocytochemical studies (Gu et al., 2009). Cells were then washed in PBS three times and incubated with Alexa-Fluor-conjugated secondary antibody (1:200; Sigma-Aldrich) for 1 h at room temperature. After washing with PBS three times, the coverslips were mounted on slides with Vectashield mounting media (Vector Laboratories, Burlingame, CA).

Labeled cells were imaged using a 100 \times objective lens with a cooled charge-coupled device camera mounted on a Nikon microscope. All specimens were imaged under identical conditions and analyzed using identical parameters. Surface NR1 clusters were measured using the ImageJ software (<http://rsbweb.nih.gov/ij/>). To define dendritic clusters, a single threshold was chosen manually so that clusters corresponded to puncta of 2-fold greater intensity than the diffuse fluorescence on the dendritic shaft. Three to four independent experiments were performed. On each coverslip, the cluster density, size, and fluorescent intensity of four to six neurons (two to three dendritic segments of 30 μ m length per neuron) were measured. Quantitative analyses were conducted blindly (without knowledge of experimental treatment).

Results

Blocking PIP₂ Synthesis Inhibits NMDAR-Mediated Currents. To test whether changes in the concentration of PIP₂ at the cell membrane can affect NMDARs, we investigated the effects of pharmacological agents that interfere with PIP₂ synthesis on NMDAR-mediated currents in acutely dissociated cortical pyramidal neurons. PIP₂ in the plasma membrane is synthesized by the progressive phosphorylation of phosphatidylinositol (PI) by phosphatidylinositol-4 kinase (PI-4 kinase), and inhibition of this enzyme can potentially suppress the cellular synthesis of PIP₂ (Nakanishi et al., 1995; Meyers and Cantley, 1997).

As shown in Fig. 1, A and B, dialysis with the PI-4 kinase inhibitor wortmannin (10 μ M) caused a progressive decrease of NMDAR current amplitudes (I_{3min} , 2114.3 \pm 303.6 pA;

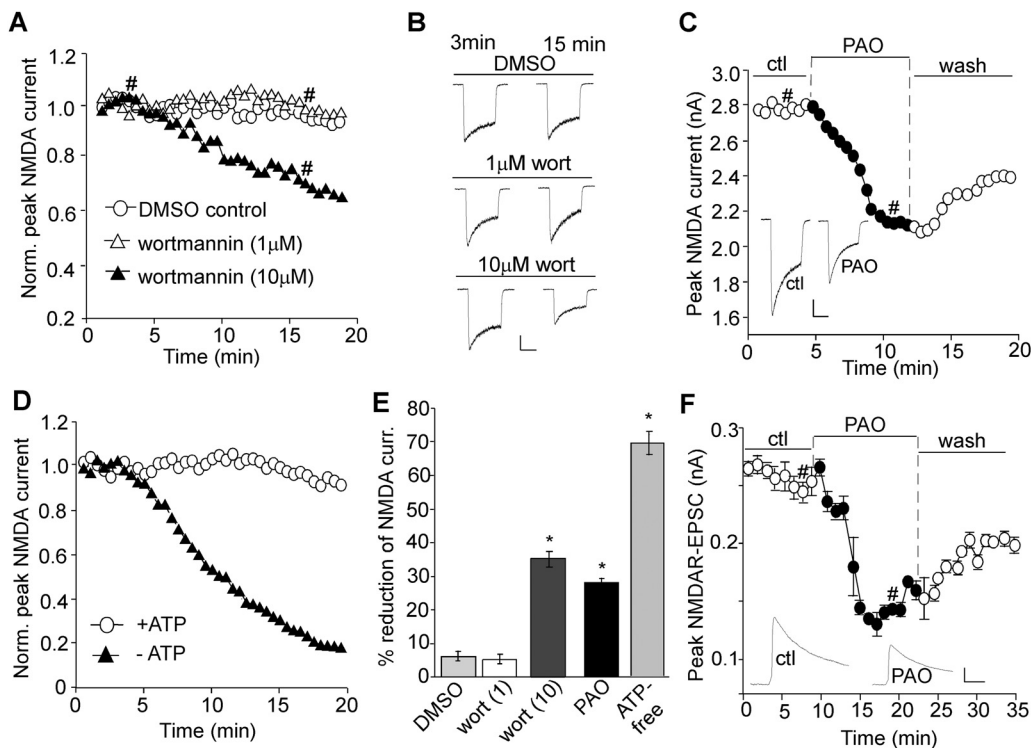


Fig. 1. Blocking PIP₂ synthesis reduces NMDAR-mediated currents. A, C, and D, plot of peak NMDA (100 μ M)-evoked currents showing the effect of wortmannin dialysis (1 and 10 μ M; A), PAO perfusion (10 μ M; C), or an ATP-free internal (D) in dissociated cortical pyramidal neurons. B and C (inset), representative current traces (at 3 and 15 min denoted by #). Scale bars, 0.5 nA, 1 s. E, cumulative data (mean \pm S.E.) showing the percentage reduction of NMDAR currents by various agents; *, $p < 0.001$, ANOVA, compared with DMSO control. F, plot of NMDAR-EPSC in cortical slices showing the effect of PAO (10 μ M) perfusion. Each point represents the average peak (mean \pm S.E.) of three consecutive NMDAR-EPSCs. Inset, representative NMDAR-EPSC traces (at time points denoted by #). Scale bars, 0.05 nA, 50 ms.

$I_{15\text{min}}$, 1337.4 ± 155.6 pA, $n = 7$). The reduction reached a steady and significant ($p < 0.001$) level after 15 min of dialysis (average reduction, $35.1 \pm 2.5\%$; Fig. 1E) compared with dialysis with DMSO control ($I_{3\text{min}}$, 2081.2 ± 375.2 pA, $I_{15\text{min}}$, 1968.3 ± 360.4 pA; $n = 7$; average reduction, $6.0 \pm 1.4\%$). Because a high concentration of wortmannin blocks both PI-3 and PI-4 kinases (Nakanishi et al., 1995; Balla et al., 1997), we also dialyzed neurons with a low concentration (1 μM) of wortmannin, at which it inhibits only PI-3 but not PI-4 kinase. At this concentration, wortmannin caused little reduction of NMDAR current amplitudes ($I_{3\text{min}}$: 1991.2 ± 287.1 pA; $I_{15\text{min}}$, 1905.7 ± 279.8 pA; $n = 6$; average reduction, $4.4 \pm 1.3\%$; Fig. 1E), which was similar to DMSO control.

We also examined the effect of wortmannin on NMDAR current decay time constant (τ). Dialysis with DMSO caused a significant ($p < 0.01$) decrease of τ over time ($\tau_{3\text{min}}$, 717.5 ± 94.1 ms; $\tau_{15\text{min}}$, 572.6 ± 78.2 ms, $n = 7$; average reduction, $24.0 \pm 3.7\%$), which is presumably due to the inactivation of NMDAR channels caused by Ca^{2+} influx and calmodulin activation (Zhang et al., 1998). A similar decrease of τ was found with 1 μM wortmannin dialysis ($\tau_{3\text{min}}$, 838.6 ± 76.8 ms; $\tau_{15\text{min}}$, 644.6 ± 64.0 ms, $n = 6$; average reduction, $23.1 \pm 3.6\%$) or 10 μM wortmannin dialysis ($\tau_{3\text{min}}$, 826.8 ± 102.8 ms; $\tau_{15\text{min}}$, 611.5 ± 100.6 ms, $n = 7$; average reduction, $26.3 \pm 6.1\%$). No significant difference in the decrease rate of τ ($\tau_{15\text{min}}/\tau_{3\text{min}}$) was observed between the control groups and groups dialyzed with wortmannin, suggesting that wortmannin did not alter the kinetics of NMDAR current.

Wortmannin is also known to inhibit myosin light chain kinase (Nakanishi et al., 1992); thus, to ensure the specific involvement of PI-4 kinase, we tested another chemically distinct inhibitor of PI-4 kinase, PAO. PAO inhibits the synthesis of PIP_2 from PI, thus lowering the membrane concentration of PIP_2 (Wiedemann et al., 1996; Várnai and Balla, 1998). As shown in Fig. 1C, bath application of PAO (10 μM) caused a significant ($p < 0.001$) reduction of NMDAR current amplitudes (I_{control} , 2746.7 ± 234.4 pA; I_{PAO} , 1991.8 ± 191.9 pA, $n = 12$; average reduction, $28.2 \pm 1.2\%$; Fig. 1E). This effect of PAO was only partially reversible.

Hydrolyzable ATP is required for the continuous synthesis of PIP_2 at the membrane (Suh and Hille, 2002); thus, we tested whether a lack of ATP affects NMDAR currents. As shown in Fig. 1D, NMDAR currents recorded with an ATP-lacking internal solution showed a marked decrease ($I_{3\text{min}}$, 1553.7 ± 265.3 pA; $I_{15\text{min}}$, 465.3 ± 93.8 pA; $n = 7$; average reduction, $69.5 \pm 2.9\%$; Fig. 1E), whereas dialysis with normal internal solution containing 3 mM ATP produced stable

NMDAR currents ($I_{3\text{min}}$, 1941.8 ± 365.0 pA; $I_{15\text{min}}$, 1761.6 ± 299.1 pA, $n = 7$; average reduction, $7.3 \pm 1.9\%$). This is consistent with a previous study showing the requirement of intracellular ATP for cortical neuronal NMDA responses (MacDonald et al., 1989).

Because whole-cell NMDAR currents in isolated neurons are mediated by both synaptic and extrasynaptic receptors, we further investigated the effect of PIP_2 on synaptic NMDAR responses. Excitatory postsynaptic currents evoked by stimulation of synaptic NMDARs (NMDAR-EPSCs) were recorded in cortical slices. As shown in Fig. 1F, PAO application induced a significant ($p < 0.001$) reduction of the NMDAR-EPSC amplitude (EPSC_{control}, 250.5 ± 25.1 pA; EPSC_{PAO}, 146.5 ± 12.1 pA, $n = 9$; average reduction, $40.1 \pm 2.4\%$). This effect of PAO was robust and only partially reversible (30–40%) after prolonged washing, suggesting that inhibition of PIP_2 synthesis can produce a long-lasting effect on synaptic NMDA receptors.

Stimulating PIP_2 Hydrolysis Inhibits NMDAR Currents. To further explore the role of PIP_2 , we examined the effect of PIP_2 hydrolysis on NMDAR currents. M1 muscarinic receptors couple to the heterotrimeric G-protein $G_{q/11}$ and subsequently activate PLC- β (Peralta et al., 1988; Rebecchi and Pentylala, 2000; Suh and Hille, 2002). PLC- β hydrolyzes PIP_2 into two second messengers, diacylglycerol (DAG) and inositol 1,4,5-triphosphate (IP_3) (Lajat et al., 1998; Rebecchi and Pentylala, 2000). Given the wide distribution of M1 muscarinic receptors in cortical neurons (Levey et al., 1991; Wei et al., 1994), we used the M1 muscarinic agonist carbachol to trigger PIP_2 hydrolysis and therefore decrease the PIP_2 content. As shown in Fig. 2A, application of carbachol (CCh, 20 μM) caused a significant ($p < 0.01$) reduction of NMDAR currents (I_{control} , 1873.8 ± 293.3 pA; I_{CCh} , 1328.9 ± 194.3 pA, $n = 7$; average reduction, $28.5 \pm 2.9\%$; Fig. 2C). As with PAO, the effect of carbachol was only partially reversible. It suggests that once PIP_2 is broken down by activated PLC- β , it produces a long-lasting effect on NMDAR currents and does not recover until PIP_2 is resynthesized at the membrane.

To confirm the involvement of PLC, we applied the PLC inhibitor U73122. As shown in Fig. 2, B and C, U73122 (10 μM) caused a significant ($p < 0.01$) increase of NMDAR currents (I_{control} , 1098.8 ± 206.3 pA; I_{U73122} , 1562.2 ± 309.0 pA, $n = 7$; average increase, $41.6 \pm 3\%$), whereas its inactive analog U73343 (10 μM) failed to change NMDAR currents (I_{control} , 1108.7 ± 155.1 pA; I_{U73343} , 1145.0 ± 166.8 pA, $n = 5$; average increase, $2.9 \pm 0.8\%$). These results suggest that

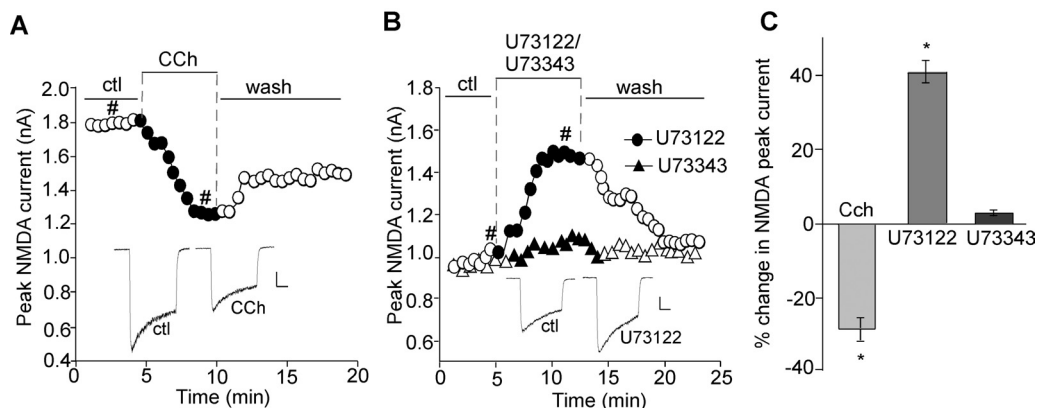


Fig. 2. Stimulating PIP_2 hydrolysis reduces NMDA-mediated currents. A and B, plot of peak NMDAR currents in cortical pyramidal neurons showing the effect of the M1 mAChR agonist carbachol (CCh, 20 μM ; A) or the PLC inhibitor U73122 (10 μM) versus the inactive analog U73343 (10 μM ; B). Inset, representative current traces (at time points denoted by #). Scale bars, 0.25 nA, 0.5 s. C, cumulative data (mean \pm S.E.) showing the percentage changes of NMDAR currents by various agents. *, $p < 0.01$, ANOVA.

the level of PIP₂ is important for maintaining NMDAR currents.

PIP₂ Facilitates NMDAR Currents. To directly examine the role of PIP₂ in the regulation of NMDAR channels, we measured the effect of exogenous application of PIP₂ on NMDAR currents. As shown in Fig. 3, A and B, dialysis with PIP₂ (20 μM) caused a significant ($p < 0.001$) increase of NMDAR currents ($I_{3\text{min}}$, 1016.9 ± 118.2 pA; $I_{20\text{min}}$, 1505.4 ± 199.2 pA, $n = 7$; average increase, 46.7 ± 6.3%; Fig. 3C), whereas stable currents were obtained in the absence of PIP₂ within the same time frame ($I_{3\text{min}}$, 1065.1 ± 163.2 pA; $I_{20\text{min}}$, 932.3 ± 29.7 pA, $n = 7$; average reduction, 11.5 ± 2.2%; Fig. 3C).

Next, we examined NMDAR currents when endogenous PIP₂ is blocked with a specific antibody (Huang et al., 1998; Liou et al., 1999; Liu and Qin, 2005). As shown in Fig. 3, A and B, dialysis with PIP₂ antibody (28.5 μg/ml) caused a significant ($p < 0.001$) decrease of NMDAR currents ($I_{3\text{min}}$, 1402.6 ± 212.3 pA; $I_{20\text{min}}$, 698.7 ± 96.5 pA, $n = 6$; average reduction, 49.9 ± 1.3%; Fig. 3C) compared with heat-inactivated PIP₂ antibody ($I_{3\text{min}}$, 1982.6 ± 308.6 pA; $I_{20\text{min}}$, 1756.0 ± 302.3 pA, $n = 7$; average reduction, 12.7 ± 1.5%; Fig. 3C).

We also examined the effect of PIP₂ or PIP₂ antibody on NMDAR current decay time constant. A similar decrease of τ over time was observed in cells dialyzed with the control solution ($\tau_{3\text{min}}$, 804.1 ± 96.4 ms; $\tau_{20\text{min}}$, 612.4 ± 64.4 ms, $n = 7$; average reduction, 21.7 ± 4.8%), PIP₂ ($\tau_{3\text{min}}$, 812.4 ± 103.5 ms; $\tau_{20\text{min}}$, 585.8 ± 50.9 ms, $n = 7$; average reduction, 23.9 ± 6.2%), or PIP₂ antibody ($\tau_{3\text{min}}$, 784.7 ± 82.5 ms; $\tau_{20\text{min}}$, 570.3 ± 62.3 ms, $n = 6$; average reduction, 25.8 ± 6.3%), suggesting the lack of effect of PIP₂ on NMDAR current kinetics.

To confirm the role of PIP₂ on synaptic NMDARs, we also

tested the effects of PIP₂ and PIP₂ antibody on NMDAR-EPSCs in PFC slices. As shown in Fig. 3, D and E, dialysis with PIP₂ significantly ($p < 0.001$) enhanced NMDAR-EPSC (EPSC_{3min}, 202.5 ± 35.3 pA; EPSC_{20min}, 260.1 ± 42.4 pA, $n = 6$; average increase, 28.7 ± 1.9%; Fig. 3F) compared with control (EPSC_{3min}, 234.7 ± 47.1 pA; EPSC_{20min}, 221.0 ± 44.1 pA, $n = 6$; average reduction, 5.8 ± 4.0%; Fig. 3F). Dialysis with PIP₂ antibody significantly ($p < 0.001$) decreased NMDAR-EPSC (EPSC_{3min}, 227.5 ± 21.3 pA; EPSC_{20min}, 104.9 ± 21.4 pA, $n = 7$; average reduction, 51.2 ± 5.2%; Fig. 3F), similar to what was found on NMDAR-mediated ionic currents in isolated neurons. It suggests that the continuous presence of PIP₂ facilitates NMDAR responses at synapses.

PIP₂ Regulates the Number of Surface NMDAR Clusters on Neuronal Dendrites. To determine whether PIP₂ regulation of NMDAR currents is caused by changes in NMDAR trafficking, we performed quantitative immunostaining of surface NMDARs in cultured cortical neurons. Neurons were incubated with PAO (10 μM) or carbachol (20 μM) for 30 min. Surface NMDAR channels were assessed by immunostaining with an antibody against the NR1 extracellular N-terminal domain in nonpermeable conditions. As shown in Fig. 4, A to C, surface NR1 punctated fluorescence on dendrites were observed in control neurons, whereas these puncta were noticeably reduced in neurons treated with PAO or carbachol. Quantitative analyses (Fig. 4D) showed that PAO significantly reduced the surface NR1 cluster density (number of clusters/25 μm dendrite) (control, 14.1 ± 1.25, $n = 14$; PAO, 5.9 ± 1.4, $n = 12$; $p < 0.005$), and cluster size (measured in square micrometers) (control, 0.38 ± 0.05; PAO, 0.14 ± 0.06; $p < 0.005$). The fluorescence intensity of surface NR1 clusters remained largely unchanged (control, 93.8 ± 0.9; PAO, 89.9 ± 1.0). Likewise, carbachol significantly diminished the surface NR1 cluster density (7.2 ± 1.8,

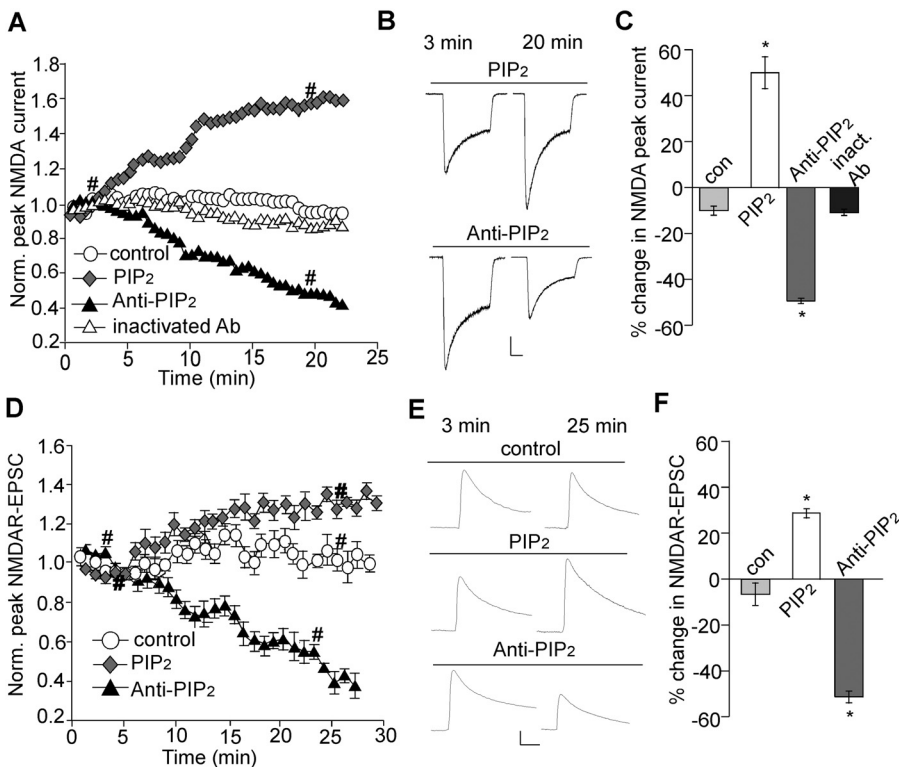


Fig. 3. PIP₂ increases channel activity. A and D, plot of NMDAR ionic currents (A) or NMDAR-EPSC (D) showing the effect of dialysis with PIP₂ (20 μM) or a PIP₂ antibody (Ab-PIP₂, 28.5 μg/ml). The heat-inactivated PIP₂ antibody (28.5 μg/ml) was used as a control. B and E, representative traces (at time points denoted by #). Scale bar, 0.25 nA, 0.5 s (B); 0.05 nA, 50 ms (E). C and F, cumulative data (mean ± S.E.) showing the percentage change of NMDAR currents (C) and NMDAR-EPSC (F) by PIP₂ and PIP₂ antibody. *, $p < 0.001$, ANOVA, compared with control.

$n = 11$) and size (0.16 ± 0.02 , $n = 11$) but not fluorescence intensity (91.1 ± 1.0 , $n = 11$). These data suggest that a loss of PIP_2 at the cell membrane, either by inhibiting its synthesis or by increasing its hydrolysis, reduces the surface expression of NMDARs.

PIP₂ Regulation of NMDAR Currents Involves Clathrin/Dynamin-Dependent Internalization of NMDARs. Surface NMDA receptors are internalized via the clathrin/dynamin-dependent mechanism (Roche et al., 2001). To determine whether the decrease of NMDAR channel currents and surface expression by loss of PIP_2 occurs as a result of enhanced NMDAR internalization, we dialyzed neurons with a dynamin inhibitory peptide, QVPSRPNRAP. This peptide is known to interfere with the binding of amphiphysin with dynamin, thereby preventing endocytosis (Gout et al., 1993). As shown in Fig. 5, A and B, the reducing effect of PAO on NMDAR currents was largely blocked in neurons dialyzed with 50 μM dynamin inhibitory peptide (I_{control} , 1208.5 ± 167.6 pA; I_{PAO} , 1141.8 ± 146.6 pA, $n = 9$; average reduction, $4.9 \pm 1.7\%$; Fig. 5C), whereas a scrambled control peptide, RNPAQRPVPS, failed to alter the effect of PAO (I_{control} , 1568 ± 328.0 pA; I_{PAO} , 1168.5 ± 247.8 pA, $n = 7$; average reduction, $24.9 \pm 1.8\%$; Fig. 5C). It suggests that PIP_2 regulation of NMDAR currents is caused by a change in clathrin/dynamin-dependent endocytosis of surface NMDARs.

PIP₂ Regulates NMDAR Internalization through an Actin/Cofilin-Dependent Mechanism. Emerging evidence suggests that cytoskeletal molecules, such as actin and microtubules, are critically involved in the trafficking of membrane proteins (Rogers and Gelfand, 2000). It has been

found that NMDAR channels are strongly regulated by the integrity of F-actin, and actin depolymerization reduces the number of functional NMDARs on the surface and at synapses (Rosenmund and Westbrook, 1993; Allison et al., 1998). On the other hand, it has been found that PIP_2 plays a key role in restructuring and maintaining actin cytoskeleton by promoting actin branching, impairing actin severing proteins, uncapping actin filaments for the addition of new monomers, and regulating proteins that promote anchoring of actin cytoskeleton to the plasma membrane (Sechi and Wehland, 2000; Yin and Janmey, 2003). Thus, we tested whether the PIP_2 regulation of NMDAR internalization is through an actin-dependent mechanism.

First, we compared the effect of PAO on NMDAR currents in the presence of agents that alter actin depolymerization. As shown in Fig. 6A, in neurons pretreated with the actin depolymerizer latrunculin B (5 μM , 30 min), PAO had a much smaller effect on NMDAR currents (I_{control} , 684.9 ± 102.0 pA; I_{PAO} , 672.9 ± 102.6 pA, $n = 7$; average reduction, $1.6 \pm 1.5\%$; Fig. 6B) compared with untreated neurons (I_{control} , 1368.0 ± 179.6 pA; I_{PAO} , 984.3 ± 132.5 pA, $n = 7$; average reduction, $28.2 \pm 1.6\%$; Fig. 6B). Note that the basal current amplitude of latrunculin-treated neurons was significantly ($p < 0.01$) smaller than that of untreated neurons, suggesting that a loss of F-actin results in a loss of functional NMDARs. Consistent with this, when latrunculin B was directly applied to neurons under recording, it reduced NMDAR currents by $\sim 50\%$, and subsequent addition of PAO did not cause any further reduction (data not shown). On the other hand, dialysis with the F-actin stabilizer phalloidin (2 μM) largely blocked the effect of PAO on NMDAR currents (Fig. 6C) (I_{control} , 1492.0 ± 300.2 pA; I_{PAO} , 1416.5 ± 289.9 pA, $n = 8$; average reduction, $4.9 \pm 1.1\%$; Fig. 6D) compared with dialysis with the normal internal solution (Fig. 6C) (I_{control} , 1652.2 ± 310.2 pA; I_{PAO} , 1232.5 ± 234.3 pA, $n = 7$; average reduction, $25.0 \pm 2.3\%$; Fig. 6D).

Actin depolymerization is regulated by multiple proteins, one of which is cofilin, a major actin depolymerizing factor (Sarmiere and Bamberg, 2004; DesMarais et al., 2005). It is noteworthy that actin and PIP_2 have been demonstrated to bind to cofilin at the same site (Yonezawa et al., 1990). PIP_2 competitively inhibits actin binding to cofilin (Yonezawa et al., 1991a,b), and cofilin remains preferentially bound to PIP_2 when PIP_2 is present (Kusano et al., 1999). We speculate that the loss of PIP_2 enables actin depolymerization by releasing the bound cofilin, leading to NMDAR current reduction. To test this, we dialyzed neurons with an antibody against cofilin to block the function of endogenous cofilin (Chan et al., 2000; Pendleton et al., 2003). As shown in Fig. 6E, the effect of PAO on NMDAR currents was significantly attenuated by the 50 μM cofilin antibody (I_{control} , 1611.7 ± 343.2 pA; I_{PAO} , 1447.9 ± 309.1 pA, $n = 8$; average reduction, $10.6 \pm 1.4\%$; Fig. 6F) but not by the heat-inactivated cofilin antibody (I_{control} , 1795.7 ± 198.1 pA; I_{PAO} , 1317.3 ± 121.0 pA, $n = 9$; average reduction, $25.6 \pm 1.9\%$; Fig. 6F). These results suggest that the PIP_2 regulation of NMDAR trafficking is through a mechanism depending on the cofilin-regulated actin dynamics.

PIP₂ Regulation of NMDAR Currents Is Impaired by A β . Reduced levels of PIP_2 have been found in the frontal cortex of AD brains (Stokes and Hawthorne, 1987; Berman et al., 2008). Moreover, oligomeric amyloid- β ($\text{A}\beta$) peptide is

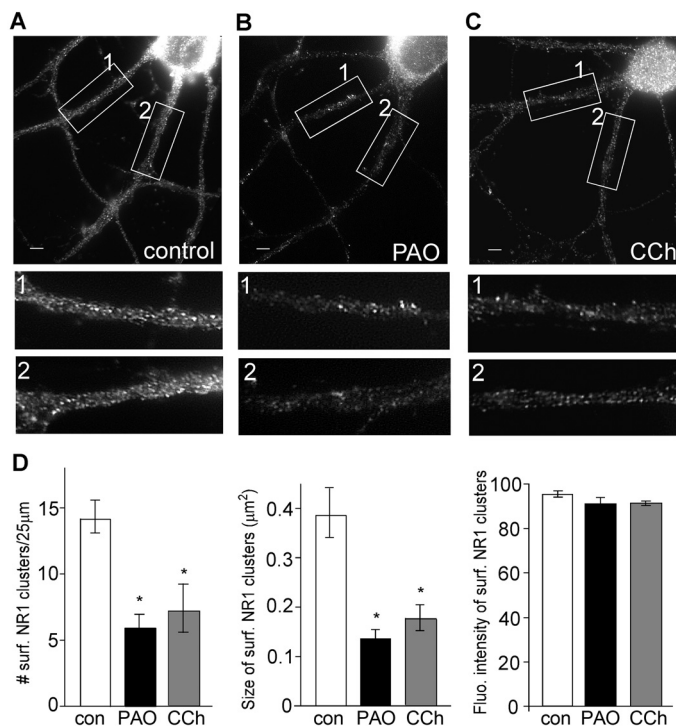


Fig. 4. Blocking PIP_2 synthesis or stimulating PIP_2 hydrolysis decreases the surface NMDAR clusters on dendrites. A to C, immunocytochemical images of surface NR1 in cortical cultures treated without (control; A) or with PAO (10 μM ; B) and carbachol (20 μM ; C). Scale bars (A–C), 5 μm . Magnified versions of the boxed regions of dendrites (numbered 1 and 2) are shown beneath each image. D, quantitative analysis of surface NR1 clusters (density, size, and intensity) along dendrites under different treatments. *, $p < 0.005$, ANOVA, compared with control.

known to disrupt PIP₂ metabolism in a Ca²⁺-dependent manner (Stokes and Hawthorne, 1987; Berman et al., 2008). Thus, we examined whether the PIP₂ regulation of NMDAR channels is altered in AD-related conditions. As shown in Fig. 7, A and B, in neurons treated with A β (1 μ M, 60 min), PAO failed to reduce NMDAR currents (I_{control} , 1047.9 \pm

151.7 pA; I_{PAO} , 1008.0 \pm 145.8 pA, $n = 7$; average reduction, 3.1 \pm 1.4%; Fig. 7C) in contrast to the effect of PAO in untreated neurons (I_{control} , 1434.4 \pm 125.5 pA; I_{PAO} , 1085.0 \pm 117.4 pA, $n = 7$; average reduction, 25.0 \pm 2.9%; Fig. 7C). These results are in agreement with our expectation that A β pretreatment disrupts basal levels of cellular PIP₂

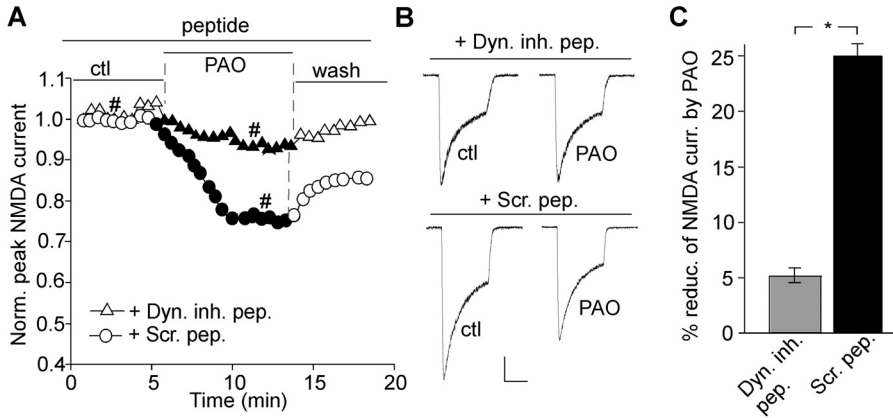


Fig. 5. Blocking PIP₂ synthesis induces NMDAR internalization via a dynamin-dependent mechanism. A, plot of normalized peak NMDAR currents showing the effect of PAO (10 μ M) in neurons dialyzed with the dynamin inhibitory peptide (50 μ M) versus a scrambled control peptide (Scr. pep., 50 μ M). B, representative current traces used to construct A (at time points denoted by #). Scale bar, 0.25 nA, 1 s. C, cumulative data (mean \pm S.E.) showing the percentage reduction of NMDAR currents by PAO in the presence of different peptides. *, $p < 0.001$, t test.

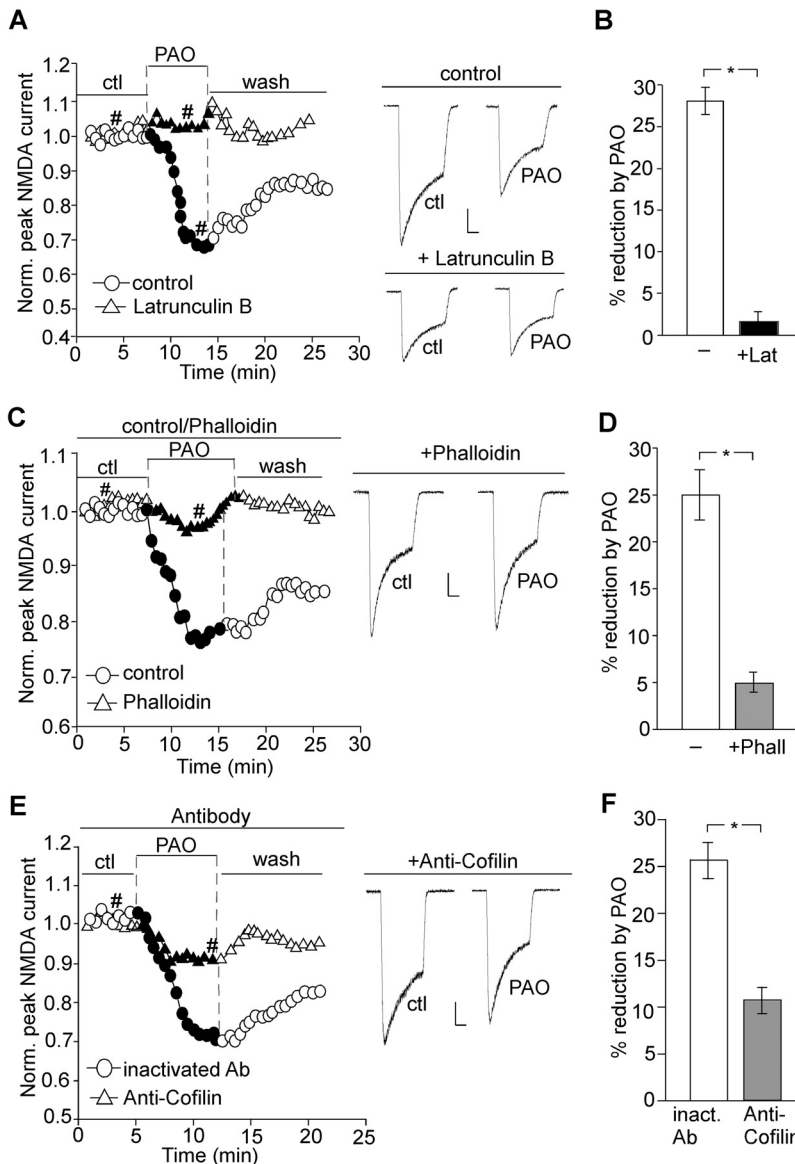


Fig. 6. PIP₂ regulation of NMDAR currents involves actin and the major depolymerizing factor cofilin. A, C, and E, plot of normalized peak NMDAR currents showing the effect of PAO (10 μ M) in neurons treated with the actin destabilizer latrunculin B (5 μ M, 30 min; A), or dialyzed with the actin stabilizer phalloidin (10 μ M; C), or dialyzed with the cofilin antibody (50 μ M; E). The heat-inactivated antibody was used as a control. Inset, representative current traces (at time points denoted by #). Scale bars, 0.25 nA, 0.5 s. B, D, and F, cumulative data (mean \pm S.E.) showing the percentage reduction of NMDAR currents by PAO in the presence of various agents. *, $p < 0.001$, t test.

(Berman et al., 2008), which might explain why no further modulation by PAO is observed.

We further validated these in vitro findings in an animal model of AD, with the transgenic mice overexpressing mutant APP. As shown in Fig. 7, D and E, PAO failed to cause a reduction of NMDAR currents in cortical neurons from APP transgenic mice (I_{control} , 1334.8 ± 177.6 pA; I_{PAO} , 1291.1 ± 178.8 pA, $n = 11$; average reduction, $3.6 \pm 1.1\%$; Fig. 7F), which was significantly ($p < 0.001$) different from the effect of PAO in neurons from wild-type mice (I_{control} , 1636.0 ± 213.5 pA; I_{PAO} , 1221.3 ± 149.8 pA, $n = 8$; average reduction, $24.6 \pm 1.5\%$; Fig. 7F). These results suggest that the PIP_2 regulation of NMDAR channels is lost in AD, probably because of the disrupted PIP_2 metabolism by $\text{A}\beta$.

Discussion

In this study, we have provided electrophysiological evidence demonstrating that the NMDAR response is regulated by the increase or decrease of PIP_2 concentrations in cortical neurons. Blocking PIP_2 synthesis or stimulating PIP_2 hydrolysis reduces NMDAR-mediated currents, whereas inhibition of PLC or exogenous application of PIP_2 enhances NMDAR currents. The PIP_2 regulation of NMDAR responses seems to be attributable to NMDAR internalization via the clathrin/dynamin-dependent mechanism. We have further demonstrated that the PIP_2 -induced change in NMDAR endocytosis is probably caused by the change in actin depolymerization that is regulated by cofilin.

Based on these results, we propose a model (Fig. 8) that schematically represents the potential mechanism by which PIP_2 influences the number of surface NMDA receptors in native neurons. Under basal conditions, PI(4)P5 kinase uses cellular ATP to convert PI(4)P to PIP_2 . As long as the rate of

PIP_2 synthesis is unperturbed and PIP_2 concentration in the plasma membrane is high, cofilin remains bound to PIP_2 preferentially over actin, and thus is unable to depolymerize F-actin. With the actin cytoskeleton intact at the PSD, NMDAR channels are stabilized at the synaptic membrane by binding to adaptor proteins like α -actinin (Wyszynski et al., 1997; Michailidis et al., 2007). Activation of PLC causes the hydrolysis of PIP_2 into DAG and IP_3 , leading to the release of cofilin, which now becomes available to bind to F-actin and depolymerize it. With the actin cytoskeleton disintegrated, NMDA receptors are internalized via clathrin-coated pits, causing the reduction of NMDAR responses. Activation of many G_q -coupled receptors, such as M1 muscarinic receptors (mAChRs) and group I metabotropic glutamate receptors, trigger PLC activation and PIP_2 hydrolysis; thus, these receptors may suppress NMDAR responses via the common PIP_2 -dependent mechanism. It provides a potential explanation for mAChR- and metabotropic glutamate receptors-mediated inhibition of NMDA component of glutamatergic transmission in ventral tegmental area neurons (Zheng and Johnson, 2003; Levy et al., 2006). There is the possibility that cholinergic agonists like carbachol modulate NMDAR currents via intracellular Ca^{2+} release and PKC activation. However, it has been demonstrated that PIP_2 hydrolysis by stimulation of PLC-coupled receptors still inhibits NR1/NR2A currents even in cells pretreated with thapsigargin, the drug that depletes Ca^{2+} from intracellular stores and suppresses NR1/2C currents, which are insensitive to regulation by PKC (Michailidis et al., 2007). Thus, the effect of carbachol on NMDAR currents is probably caused by PIP_2 hydrolysis.

Because reducing PIP_2 levels causes the internalization of NMDARs from the plasma membrane, PIP_2 must act to

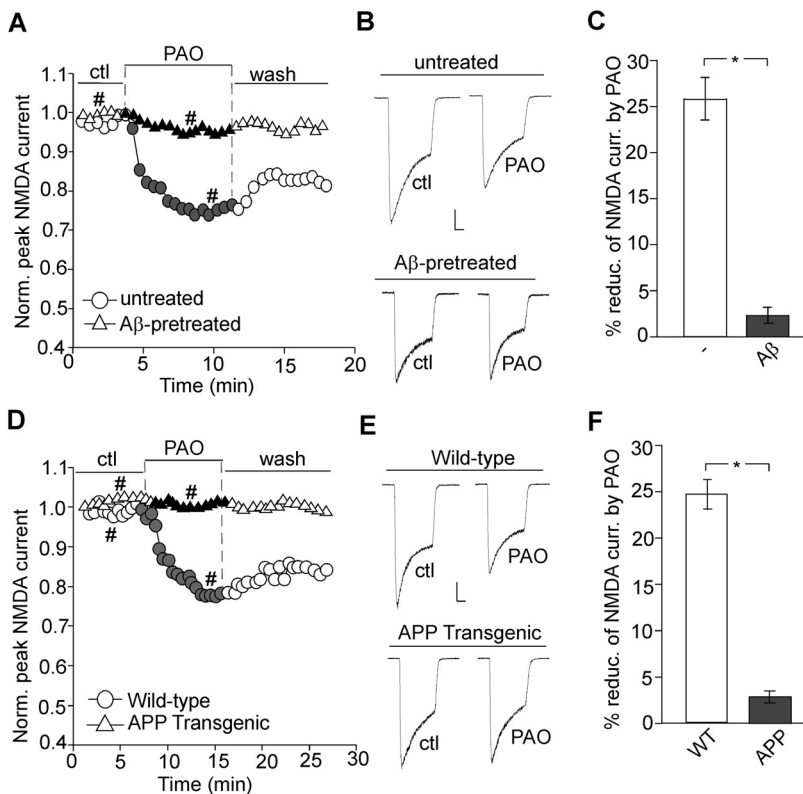


Fig. 7. PIP_2 regulation of NMDAR channels is abolished by $\text{A}\beta$ and in APP transgenic mice. A and D, plot of normalized peak NMDAR currents showing the effect of PAO (10 μM) in cultured cortical neurons pretreated with or without $\text{A}\beta$ oligomer (1 μM , 60 min; A) or in neurons isolated from APP transgenic versus wild-type mice (D). B and E, representative current traces (at time points denoted by #). Scale bars, 0.25 nA, 0.5 s. C and F, cumulative data (mean \pm S.E.) showing the percentage of reduction of NMDAR currents by PAO in neurons treated with $\text{A}\beta$ or from APP transgenic mice. *, $p < 0.001$, t test.

interfere with some key factor(s) that facilitates NMDAR endocytosis. Actin is a likely candidate because of its involvement in maintaining the surface/synaptic localization and function of NMDARs (Rosenmund and Westbrook, 1993; Allison et al., 1998; Morishita et al., 2005). Moreover, PIP₂ has been found to play a critical role in modulating actin dynamics (Takenawa and Itoh, 2001; Yin and Janmey, 2003). Increased cellular PIP₂ by overexpression of PI(4)5-kinase in heterologous systems can induce the formation of actin filament bundles, whereas the phosphoinositide phosphatase synaptojanin disrupts them (Allison et al., 1998; Janmey et al., 1999). PIP₂ facilitates actin polymerization by inhibiting actin capping proteins (e.g., CapZ and gelsolin), nucleotide exchange proteins (e.g., profilin), and actin filament-severing proteins (e.g., cofilin) (Janmey et al., 1999; Sechi and Wehland, 2000). In addition, PIP₂ activates cross-linking proteins (e.g., α -actinin) and proteins that bind the actin cytoskeleton to plasma membrane (e.g., vinculin and ezrin/radixin/moesin) (Sechi and Wehland, 2000; Takenawa and Itoh, 2001).

Our data suggest the involvement of cofilin in PIP₂ regulation of NMDARs in cortical neurons. The importance of cofilin in regulating actin dynamics cannot be undermined because it is the major actin depolymerizing factor abundantly distributed in the soma, axons, and dendrites of central and peripheral neurons (Sarmiere and Bamburg, 2004). Cofilin, which acts to enhance actin monomer dissociation and reduce actin-actin interactions (DesMarais et al., 2005), is tightly regulated. Apart from its regulation by phosphorylation/dephosphorylation (Huang et al., 2006; Endo et al., 2007), a separate membrane-bound pool of cofilin is regulated by its binding status to PIP₂ (Sarmiere and Bamburg, 2004; Hosoda et al., 2007; van Rheenen et al., 2007). Cofilin has a short sequence at the N terminus that is the common binding site for both PIP₂ and actin (Yonezawa et al., 1991a,b). Biochemical studies show that in the presence of PIP₂, cofilin binds preferentially to PIP₂, which inhibits its actin-binding activity (Yonezawa et al., 1991a; DesMarais et al., 2005). Thus, we speculate that active cofilin is bound to PIP₂ in an inhibitory "caged" complex in resting conditions; upon PIP₂ hydrolysis, it is "uncaged" to become available to bind to F-actin and depolymerize it. Consistent with this, it

has been found that epidermal growth factor-induced PLC activation causes the release of cofilin, leading to F-actin disintegration in carcinoma cells (van Rheenen et al., 2007).

The current knowledge about NMDAR-PIP₂ interactions is largely based on the work of Michailidis et al. (2007), who discovered that PIP₂ affects NMDAR channels through α -actinin in the *X. laevis* oocyte expression system. Our present study has investigated the intracellular mechanism underlying the regulation of native NMDARs by PIP₂ in cortical neurons. Both Michailidis et al. (2007) and we have found that PIP₂ inhibition leads to the suppression of NMDAR currents. There are a few differences between the two studies. Michailidis et al. (2007) found that PLC-catalyzed PIP₂ hydrolysis (by stimulation of epidermal growth factor receptor or M1 mAChRs) only elicited a transient inhibition of NMDAR currents, although we found that the mAChR agonist carbachol caused a sustained inhibition of NMDAR currents and only partially recovered upon washing off the drug (Fig. 2). This indicates that the effect of PIP₂ hydrolysis is long-lasting, and the NMDAR channels do not become fully functional until another biosynthetic cycle of PIP₂ is completed. As to the mechanism underlying PIP₂ regulation of NMDARs, Michailidis et al. (2007) suggest that α -actinin tethers to C-terminal regions of NMDARs and PIP₂ in the plasma membrane to keep the channel fully open; when PIP₂ is hydrolyzed by PLC, α -actinin is detached from the membrane and is no longer able to keep the channel "open," resulting in the shift of NMDAR conformation to a "restrained" state, which accounts for the suppression of the current. Our model (Fig. 8), on the other hand, demonstrated that the integrity of the actin cytoskeleton is directly linked to PIP₂ regulation of NMDAR channels. We propose that depletion of membrane PIP₂ affects the polymerization state of F-actin via cofilin, therefore affecting the membrane trafficking of NMDARs. Because F-actin is required for anchoring NMDARs at the surface/synapses (Rosenmund and Westbrook, 1993; Allison et al., 1998), decreased actin cytoskeletal support should be accompanied by enhanced internalization of NMDAR channels. This is consistent with our findings that blocking the clathrin/dynamin-dependent internalization prevents PIP₂ regulation of NMDAR currents (Fig. 5).

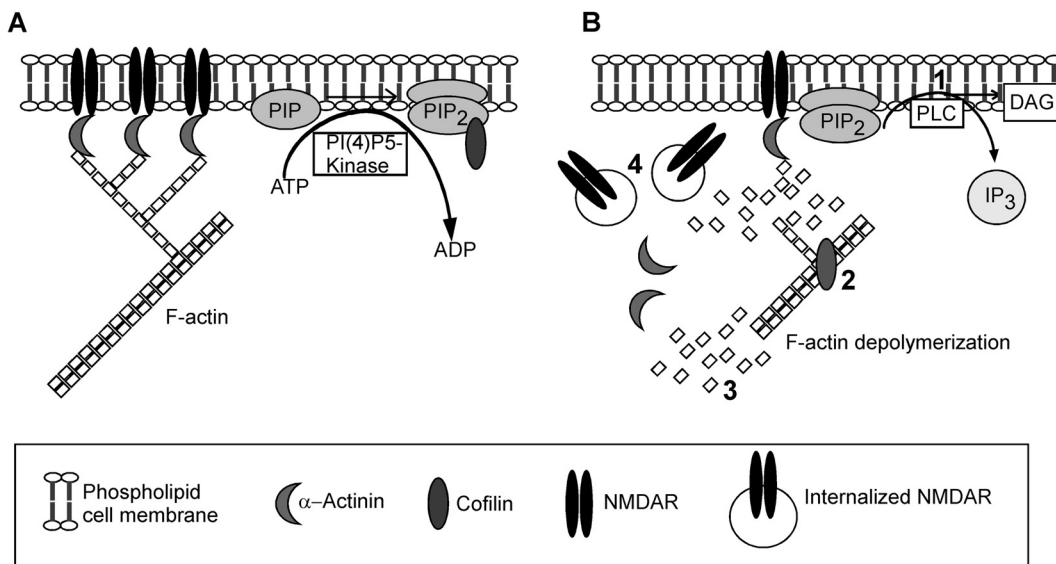


Fig. 8. A schematic model demonstrating the potential mechanism for PIP₂ regulation of NMDAR channels. **A**, PIP₂ is being constantly synthesized at the membrane by phosphorylation of PIP by PI(4) P5-kinase at the expense of ATP hydrolysis. The presence of membrane PIP₂ binds to cofilin and holds it in an inactive "caged" state, preventing its binding to F-actin. Intact actin helps maintain NMDARs at the synaptic membrane. **B**, when PIP₂ is hydrolyzed (step 1) to DAG and IP₃ by activation of PLC, cofilin is free to bind (step 2) to actin, causing depolymerization and severing (step 3) of actin filaments. With the cytoskeleton support lost, NMDAR channels are internalized (step 4), thus causing a reduction of NMDAR currents.

Thus, PIP₂ may affect the functionality of NMDAR channels in more than one way, because both PIP₂ and NMDARs are known to interact with a diverse array of molecules. It must be noted that even though our model predicts that cofilin directly binds to PIP₂, the possibility of an intermediary binding partner cannot be ignored.

The potential correlation between reduced levels of phosphoinositides in the brain and symptoms of Alzheimer's disease has been established (Stokes and Hawthorne, 1987; Landman et al., 2006; Berman et al., 2008). With the level of PIP₂ diminished by Aβ, it is not surprising that a subsequent application of PI-4 kinase inhibitors to block PIP₂ synthesis fails to exert a strong influence on NMDAR currents.

Because PIP₂ concentration on the cytosolic leaflet at the plasma membrane undergoes a constant cycle of regeneration and breakdown (Toker, 1998; Suh and Hille, 2005), it is conceivable that any perturbation of this pathway is likely to affect the functioning of ion channels that are directly or indirectly regulated by this phospholipid. Overall, our study has identified one possible mechanism by which PIP₂ regulates NMDAR channel trafficking and function in central neurons.

Acknowledgments

We thank Dr. Eunice Yuen, Dr. Ping Zhong, and Xiaoqing Chen for technical support.

References

Albert AP, Saleh SN, and Large WA (2008) Inhibition of native TRPC6 channel activity by phosphatidylinositol 4,5-bisphosphate in mesenteric artery myocytes. *J Physiol* **586**:3087–3095.

Allison DW, Gelfand VI, Spector I, and Craig AM (1998) Role of actin in anchoring postsynaptic receptors in cultured hippocampal neurons: differential attachment of NMDA versus AMPA receptors. *J Neurosci* **18**:2423–2436.

Balla T, Downing GJ, Jaffe H, Kim S, Zolyomi A, and Catt KJ (1997) Isolation and molecular cloning of wortmannin-sensitive bovine type III phosphatidylinositol 4-kinases. *J Biol Chem* **272**:18358–18366.

Berman DE, Dall'Armi C, Voronov SV, McIntire LB, Zhang H, Moore AZ, Staniszewski A, Arancio O, Kim TW, and Di Paolo G (2008) Oligomeric amyloid-beta peptide disrupts phosphatidylinositol-4,5-bisphosphate metabolism. *Nat Neurosci* **11**:547–554.

Chan AY, Bailly M, Zebda N, Segall JE, and Condeelis JS (2000) Role of cofilin in epidermal growth factor-stimulated actin polymerization and lamellipod protrusion. *J Cell Biol* **148**:531–542.

Dahlgren KN, Manelli AM, Stine WR Jr, Baker LK, Krafft GA, and LaDu MJ (2002) Oligomeric and fibrillar species of amyloid-beta peptides differentially affect neuronal viability. *J Biol Chem* **277**:32046–32053.

DesMarais V, Ghosh M, Eddy R, and Condeelis J (2005) Cofilin takes the lead. *J Cell Sci* **118**:19–26.

Dingledine R, Borges K, Bowie D, and Traynelis SF (1999) The glutamate receptor ion channels. *Pharmacol Rev* **51**:7–61.

Endo M, Ohashi K, and Mizuno K (2007) LIM kinase and slingshot are critical for neurite extension. *J Biol Chem* **282**:13692–13702.

Fukami K, Furuhashi K, Inagaki M, Endo T, Hatano S, and Takenawa T (1992) Requirement of phosphatidylinositol 4,5-bisphosphate for alpha-actinin function. *Nature* **359**:150–152.

Gout I, Dhand R, Hiles ID, Fry MJ, Panayotou G, Das P, Truong O, Totty NF, Hsuan J, and Booker GW (1993) The GTPase dynamin binds to and is activated by a subset of SH3 domains. *Cell* **75**:25–36.

Gu Z, Liu W, and Yan Z (2009) β-Amyloid impairs AMPA receptor trafficking and function by reducing Ca²⁺/calmodulin-dependent protein kinase II synaptic distribution. *J Biol Chem* **284**:10639–10649.

Hilgemann DW and Ball R (1996) Regulation of cardiac Na⁺,Ca²⁺ exchange and KATP potassium channels by PIP₂. *Science* **273**:956–959.

Horne EA and Dell'Acqua ML (2007) Phospholipase C is required for changes in postsynaptic structure and function associated with NMDA receptor-dependent long-term depression. *J Neurosci* **27**:3523–3534.

Hosoda A, Sato N, Nagaoka R, Abe H, and Obinata T (2007) Activity of cofilin can be regulated by a mechanism other than phosphorylation/dephosphorylation in muscle cells in culture. *J Muscle Res Cell Motil* **28**:183–194.

Huang CL, Feng S, and Hilgemann DW (1998) Direct activation of inward rectifier potassium channels by PIP₂ and its stabilization by Gbetagamma. *Nature* **391**:803–806.

Huang TY, DerMardirossian C, and Bokoch GM (2006) Cofilin phosphatases and regulation of actin dynamics. *Curr Opin Cell Biol* **18**:26–31.

Janney PA, Xian W, and Flanagan LA (1999) Controlling cytoskeleton structure by phosphoinositide-protein interactions: phosphoinositide binding protein domains and effects of lipid packing. *Chem Phys Lipids* **101**:93–107.

Kobrinisky E, Mirshahi T, Zhang H, Jin T, and Logothetis DE (2000) Receptor-mediated hydrolysis of plasma membrane messenger PIP₂ leads to K⁺-current desensitization. *Nat Cell Biol* **2**:507–514.

Kornau HC, Schenker LT, Kennedy MB, and Seeburg PH (1995) Domain interaction between NMDA receptor subunits and the postsynaptic density protein PSD-95. *Science* **269**:1737–1740.

Kunzelmann K, Bachhuber T, Regeer R, Markovich D, Sun J, and Schreiber R (2005) Purinergic inhibition of the epithelial Na⁺ transport via hydrolysis of PIP₂. *FASEB J* **19**:142–143.

Kusano K, Abe H, and Obinata T (1999) Detection of a sequence involved in actin-binding and phosphoinositide-binding in the N-terminal side of cofilin. *Mol Cell Biochem* **190**:133–141.

Lajlat S, Harbon S, and Tanfin Z (1998) Carbachol-induced desensitization of PLC-beta pathway in rat myometrium: downregulation of Gqalpha/G11alpha. *Am J Physiol* **275**:C636–C645.

Landman N, Jeong SY, Shin SY, Voronov SV, Serban G, Kang MS, Park MK, Di Paolo G, Chung S, and Kim TW (2006) Presenilin mutations linked to familial Alzheimer's disease cause an imbalance in phosphatidylinositol 4,5-bisphosphate metabolism. *Proc Natl Acad Sci U S A* **103**:19524–19529.

Lau CG and Zukin RS (2007) NMDA receptor trafficking in synaptic plasticity and neuropsychiatric disorders. *Nat Rev Neurosci* **8**:413–426.

Levey AI, Kitt CA, Simonds WF, Price DL, and Brann MR (1991) Identification and localization of muscarinic acetylcholine receptor proteins in brain with subtype-specific antibodies. *J Neurosci* **11**:3218–3226.

Levy RB, Reyes AD, and Aoki C (2006) Nicotinic and muscarinic reduction of unitary excitatory postsynaptic potentials in sensory cortex: dual intracellular recording in vitro. *J Neurophysiol* **95**:2155–2166.

Lin Y, Skeberdis VA, Francesconi A, Bennett MV, and Zukin RS (2004) Postsynaptic density protein-95 regulates NMDA channel gating and surface expression. *J Neurosci* **24**:10138–10148.

Liou HH, Zhou SS, and Huang CL (1999) Regulation of ROMK1 channel by protein kinase A via a phosphatidylinositol 4,5-bisphosphate-dependent mechanism. *Proc Natl Acad Sci U S A* **96**:5820–5825.

Liu B and Qin F (2005) Functional control of cold- and menthol-sensitive TRPM8 ion channels by phosphatidylinositol 4,5-bisphosphate. *J Neurosci* **25**:1674–1681.

MacDonald JF, Mody I, and Salter MW (1989) Regulation of N-methyl-D-aspartate receptors revealed by intracellular dialysis of murine neurones in culture. *J Physiol* **414**:17–34.

Meyers R and Cantley LC (1997) Cloning and characterization of a wortmannin-sensitive human phosphatidylinositol 4-kinase. *J Biol Chem* **272**:4384–4390.

Michailidis IE, Helton TD, Petrou VI, Mirshahi T, Ehlers MD, and Logothetis DE (2007) Phosphatidylinositol-4,5-bisphosphate regulates NMDA receptor activity through alpha-actinin. *J Neurosci* **27**:5523–5532.

Morishita W, Marie H, and Malenka RC (2005) Distinct triggering and expression mechanisms underlie LTD of AMPA and NMDA synaptic responses. *Nat Neurosci* **8**:1043–1050.

Nakanishi S, Catt KJ, and Balla T (1995) A wortmannin-sensitive phosphatidylinositol 4-kinase that regulates hormone-sensitive pools of inositolphospholipids. *Proc Natl Acad Sci U S A* **92**:5317–5321.

Nakanishi S, Kakita S, Takahashi I, Kawahara K, Tsukuda E, Sano T, Yamada K, Yoshida M, Kase H, and Matsuda Y (1992) Wortmannin, a microbial product inhibitor of myosin light chain kinase. *J Biol Chem* **267**:2157–2163.

Pak DT, Yang S, Rudolph-Correia S, Kim E, and Sheng M (2001) Regulation of dendritic spine morphology by SPAR, a PSD-95-associated RapGAP. *Neuron* **31**:289–303.

Pendleton A, Pope B, Weeds A, and Koffer A (2003) Latrunculin B or ATP depletion induces cofilin-dependent translocation of actin into nuclei of mast cells. *J Biol Chem* **278**:14394–14400.

Peralta EG, Ashkenazi A, Winslow JW, Ramachandran J, and Capon DJ (1988) Differential regulation of PI hydrolysis and adenyllyl cyclase by muscarinic receptor subtypes. *Nature* **334**:434–437.

Prescott ED and Julius D (2003) A modular PIP₂ binding site as a determinant of capsaicin receptor sensitivity. *Science* **300**:1284–1288.

Prybylowski K, Chang K, Sans N, Kan L, Vicini S, and Wenthold RJ (2005) The synaptic localization of NR2B-containing NMDA receptors is controlled by interactions with PDZ proteins and AP-2. *Neuron* **47**:845–857.

Rebecchi MJ and Pentylala SN (2000) Structure, function, and control of phosphoinositide-specific phospholipase C. *Physiol Rev* **80**:1291–1335.

Roche KW, Standley S, McCallum J, Dune Ly C, Ehlers MD, and Wenthold RJ (2001) Molecular determinants of NMDA receptor internalization. *Nat Neurosci* **4**:794–802.

Rogers SL and Gelfand VI (2000) Membrane trafficking, organelle transport, and the cytoskeleton. *Curr Opin Cell Biol* **12**:57–62.

Rosenmund C and Westbrook GL (1993) Calcium-induced actin depolymerization reduces NMDA channel activity. *Neuron* **10**:805–814.

Sarmiere PD and Bamberg JR (2004) Regulation of the neuronal actin cytoskeleton by ADF/cofilin. *J Neurobiol* **58**:103–117.

Sechi AS and Wehland J (2000) The actin cytoskeleton and plasma membrane connection: PtdIns(4,5)P₂ influences cytoskeletal protein activity at the plasma membrane. *J Cell Sci* **113**:3685–3695.

Stokes CE and Hawthorne JN (1987) Reduced phosphoinositide concentrations in anterior temporal cortex of Alzheimer-diseased brains. *J Neurochem* **48**:1018–1021.

Suh BC and Hille B (2002) Recovery from muscarinic modulation of M current channels requires phosphatidylinositol 4,5-bisphosphate synthesis. *Neuron* **35**:507–520.

Suh BC and Hille B (2005) Regulation of ion channels by phosphatidylinositol 4,5-bisphosphate. *Curr Opin Neurobiol* **15**:370–378.

Takenawa T and Itoh T (2001) Phosphoinositides, key molecules for regulation of

- actin cytoskeletal organization and membrane traffic from the plasma membrane. *Biochim Biophys Acta* **1533**:190–206.
- Toker A (1998) The synthesis and cellular roles of phosphatidylinositol 4,5-bisphosphate. *Curr Opin Cell Biol* **10**:254–261.
- van Rheeën J, Song X, van Roosmalen W, Cammer M, Chen X, Desmarais V, Yip SC, Backer JM, Eddy RJ, and Condeelis JS (2007) EGF-induced PIP₂ hydrolysis releases and activates cofilin locally in carcinoma cells. *J Cell Biol* **179**:1247–1259.
- Várnai P and Balla T (1998) Visualization of phosphoinositides that bind pleckstrin homology domains: calcium- and agonist-induced dynamic changes and relationship to myo-[3H]inositol-labeled phosphoinositide pools. *J Cell Biol* **143**:501–510.
- Vissel B, Krupp JJ, Heinemann SF, and Westbrook GL (2001) A use-dependent tyrosine dephosphorylation of NMDA receptors is independent of ion flux. *Nat Neurosci* **4**:587–596.
- Wang X, Zhong P, Gu Z, and Yan Z (2003) Regulation of NMDA receptors by dopamine D4 signaling in prefrontal cortex. *J Neurosci* **23**:9852–9861.
- Washbourne P, Bennett JE, and McAllister AK (2002) Rapid recruitment of NMDA receptor transport packets to nascent synapses. *Nat Neurosci* **5**:751–759.
- Wei J, Walton EA, Milici A, and Buccafusco JJ (1994) m1–m5 muscarinic receptor distribution in rat CNS by RT-PCR and HPLC. *J Neurochem* **63**:815–821.
- Wentholt RJ, Prybylowski K, Standley S, Sans N, and Petralia RS (2003) Trafficking of NMDA receptors. *Annu Rev Pharmacol Toxicol* **43**:335–358.
- Wiedemann C, Schäfer T, and Burger MM (1996) Chromaffin granule-associated phosphatidylinositol 4-kinase activity is required for stimulated secretion. *EMBO J* **15**:2094–2101.
- Wu L, Bauer CS, Zhen XG, Xie C, and Yang J (2002) Dual regulation of voltage-gated calcium channels by PtdIns(4,5)P₂. *Nature* **419**:947–952.
- Wyszynski M, Lin J, Rao A, Nigh E, Beggs AH, Craig AM, and Sheng M (1997) Competitive binding of alpha-actinin and calmodulin to the NMDA receptor. *Nature* **385**:439–442.
- Yin HL and Janmey PA (2003) Phosphoinositide regulation of the actin cytoskeleton. *Annu Rev Physiol* **65**:761–789.
- Yonezawa N, Homma Y, Yahara I, Sakai H, and Nishida E (1991a) A short sequence responsible for both phosphoinositide binding and actin binding activities of cofilin. *J Biol Chem* **266**:17218–17221.
- Yonezawa N, Nishida E, Iida K, Kumagai H, Yahara I, and Sakai H (1991b) Inhibition of actin polymerization by a synthetic dodecapeptide patterned on the sequence around the actin-binding site of cofilin. *J Biol Chem* **266**:10485–10489.
- Yonezawa N, Nishida E, Iida K, Yahara I, and Sakai H (1990) Inhibition of the interactions of cofilin, destrin, and deoxyribonuclease I with actin by phosphoinositides. *J Biol Chem* **265**:8382–8386.
- Yuen EY, Jiang Q, Feng J, and Yan Z (2005) Microtubule regulation of N-methyl-D-aspartate receptor channels in neurons. *J Biol Chem* **280**:29420–29427.
- Yuen EY, Ren Y, and Yan Z (2008) Postsynaptic density-95 (PSD-95) and calcineurin control the sensitivity of N-methyl-D-aspartate receptors to calpain cleavage in cortical neurons. *Mol Pharmacol* **74**:360–370.
- Zhang H, Craciun LC, Mirshahi T, Rohács T, Lopes CM, Jin T, and Logothetis DE (2003) PIP₂ activates KCNQ channels, and its hydrolysis underlies receptor-mediated inhibition of M currents. *Neuron* **37**:963–975.
- Zhang S, Ehlers MD, Bernhardt JP, Su CT, and Huganir RL (1998) Calmodulin mediates calcium-dependent inactivation of N-methyl-D-aspartate receptors. *Neuron* **21**:443–453.
- Zheng F and Johnson SW (2003) Metabotropic glutamate and muscarinic cholinergic receptor-mediated preferential inhibition of N-methyl-D-aspartate component of transmissions in rat ventral tegmental area. *Neuroscience* **116**:1013–1020.

Address correspondence to: Dr. Zhen Yan, Department of Physiology and Biophysics, State University of New York at Buffalo, 124 Sherman Hall, Buffalo, NY 14214. E-mail: zhenyan@buffalo.edu
